EuroIntervention 2021;17:599-606 published online jaa December 2020

Near-infrared spectroscopy carotid plaque characteristics and cerebral embolism in carotid artery stenting

Ichiro Nakagawa[1]*, MD, PhD; Masashi Kotsugi[1], MD; Hun Soo Park[1], MD, PhD; Takanori Furuta[1], MD; Fumiya Sato[1], MD; Kaoru Myouchin[2], MD; Fumihiko Nishimura[1], MD, PhD; Shuichi Yamada[1], MD, PhD; Yasushi Motoyama[1], MD, PhD; Hiroyuki Nakase[1], MD, PhD

1. Department of Neurosurgery, Nara Medical University, Nara, Japan; 2. Department of Radiology, Nara Medical University, Nara, Japan

This paper also includes supplementary data published online at: https://eurointervention.pcronline.com/doi/10.4244/EIJ-D-20-01050

KEYWORDS

- carotid stenting
- ischaemic stroke
- MRI
- other imaging modalities
- stroke

Abstract

Background: Perioperative thromboembolism is the main consideration in carotid artery stenting (CAS). Precise evaluation of carotid plaque components is clinically important to reduce ischaemic complications since CAS mechanically pushes plaque outwards, which releases plaque debris into the bloodstream.

Aims: This study aimed to determine whether high lipid core plaque (LCP) assessed by catheter-based near-infrared spectroscopy (NIRS) is associated with ipsilateral cerebral embolism by diffusion-weighted magnetic resonance imaging during CAS using a first-generation stent.

Methods: Carotid stenosis magnetic resonance (MR) T1-weighted plaque signal intensity ratio (T1W-SIR) followed by NIRS assessment at the time of CAS (using the carotid artery Wallstent) was performed in 117 consecutive patients.

Results: The maximum lipid core burden index (max-LCBI) at minimal luminal areas (MLA; max-$LCBI_{MLA}$) and the max-LCBI for any 4 mm segment in a target lesion defined as max-$LCBI_{area}$ were significantly higher for the post-procedural new ipsilateral diffusion-weighted magnetic resonance imaging (DWI)-positive than negative patients ($p<0.001$ for all). There was a significant linear correlation between max-$LCBI_{area}$ and the number of new emboli ($r=0.544$, $p<0.0001$). We also found that the second quantile (Q2) of T1W-SIR_{MLA} had a significantly higher max-$LCBI_{MLA}$ and a higher incidence of DWI positivity than Q1 and Q3 ($p<0.001$ for all). Furthermore, max-$LCBI_{MLA}$ appeared to distinguish between patients with and without postoperative new ipsilateral DWI positivity (AUC 0.91, 95% CI: 0.86-0.96; $p<0.0001$).

Conclusions: High LCP assessed by NIRS is associated with cerebral embolism by diffusion-weighted imaging in CAS using a first-generation stent.

**Corresponding author: Department of Neurosurgery, Nara Medical University, 840 Shijo-cho, Kashihara, Nara, 634-8522, Japan. E-mail: nakagawa@naramed-u.ac.jp*

SUBMITTED ON 28/08/2020 - REVISION RECEIVED ON 1st 07/10/2020 / 2nd 26/11/2020 - ACCEPTED ON 04/12/2020

DOI: 10.4244/EIJ-D-20-01050

Abbreviations

CAS	carotid artery stenting
CEA	carotid endarterectomy
DWI	diffusion-weighted imaging
IPH	intraplaque haemorrhage
IVUS	intravascular ultrasound
LCBI	lipid core burden index
LCP	lipid core plaque
MLA	minimal lumen area
MRA	magnetic resonance angiography
MRI	magnetic resonance imaging
NIRS	near-infrared spectroscopy
SIR	signal intensity ratio
TIA	transient ischaemic attack
T1W	T1-weighted
TOF	time-of-flight

Introduction

Carotid artery stenting (CAS) has become a popular alternative to invasive carotid endarterectomy (CEA) in primary and secondary stroke prevention. Randomised trial evidence shows that CAS, despite being associated with an increased early embolic risk, is in the long term not inferior to CEA[1]. Indeed, one major concern with CAS using first-generation (single-layered) stents is incomplete plaque insulation, leading to plaque prolapse and an increased incidence of, in most cases minor, stroke[1,2]. Thus, evaluation of the carotid plaque composition may play a role in estimating the risk of embolic events during CAS[3,4]. Procedure-related multiple emboli may cause not only clinical strokes but also long-term cognitive dysfunction by subclinical embolic infarcts[5]. Silent brain infarcts on diffusion-weighted magnetic resonance imaging (MRI) are a recognised surrogate outcome measure for procedural stroke[6]. The composition of unstable plaque, including a lipid necrotic core and intraplaque haemorrhage (IPH), is commonly assessed using MRI[7]. Although a high volume of lipid core plaque (LCP) is the main risk factor for myocardial infarct during stent deployment[8], unstable carotid plaques often contain IPH, and the increased risk of embolism during CAS might depend on the lipid component[9]. Recent catheter-based near-infrared spectroscopy (NIRS) can detect LCP in coronary arteries, and NIRS of a non-culprit vessel in patients with coronary artery disease predicts increased risk of cardiovascular events[10,11]. LCP has recently been detected in carotid arteries using NIRS[12,13] and has confirmed histological validation[14]; however, its value in terms of CAS deployment remains unknown. The present study aimed to determine whether high LCP assessed by NIRS can define increased risk of embolic infarct by diffusion-weighted imaging (DWI) in CAS.

Methods

STUDY DESIGN

This prospective observational study was based on criteria of the STROBE (Strengthening the Reporting of Observational Studies in Epidemiology) statement. This study analysed LCP assessed by NIRS during CAS at a single centre between 2017 and 2020.

INCLUSION CRITERIA

We prospectively recruited 117 consecutive patients who underwent CAS to treat internal carotid artery stenosis at our institute between April 2017 and March 2020. The inclusion criteria comprised >80% stenosis in asymptomatic lesions, and >50% stenosis in symptomatic lesions accompanied by ipsilateral acute cerebral infarction or transient ischaemic attack (TIA), and high risk for CEA according to the Stenting and Angioplasty with Protection in Patients at High Risk for Endarterectomy (SAPPHIRE) criteria[15]. Patients with carotid artery occlusion requiring thrombolysis or thrombectomy were excluded.

Two antiplatelet agents (aspirin 100 mg, clopidogrel 75 mg, or cilostazol 200 mg) and statins (rosuvastatin 5 mg/day, pitavastatin 4 mg/day, or atorvastatin 10 mg/day) were administered to all patients starting four weeks before CAS. Platelet function in all patients was analysed using the VerifyNow rapid platelet function assay (Accumetrics, San Diego, CA, USA) on the day before undergoing CAS.

Baseline clinical characteristics recorded for each patient included patient age, sex, history of risk factors, and preoperative medical conditions. Hyperlipidaemia was defined as serum low-density lipoprotein cholesterol (LDL-C) ≥120 mg/dL. Patients with diabetes mellitus were included if they had been medically managed for at least two months without changes in their hypoglycaemic treatment regimens. Chronic kidney disease (CKD) was determined as an estimated glomerular filtration rate (eGFR) <60 mL/min/1.73 m^2. Current smokers were defined as those who had smoked at least one cigarette per day during the month before CAS. All patients underwent preoperative MRI/angiography and duplex sonography, followed by digital subtraction angiography.

The institutional review board at our university approved the study protocol (Approval no. 1456). All patients provided written, informed consent to their participation in all CAS procedures and allowed access to their medical records for research purposes.

INTERVENTION

An activated clotting time of >275 s was maintained using intravenous heparin during CAS procedures under local anaesthesia. An 8 Fr guiding catheter was placed in the common carotid artery. A stenotic lesion was then crossed using a guidewire. Then a FilterWire EZ™ embolic protection device (Boston Scientific, Marlborough, MA, USA) was inserted distal to the lesion. The flow was reversed under proximal guiding balloon protection for severely stenotic and/or thrombus-containing lesions because of the high potential for distal embolism when an embolic protection filter passes through the stenotic lesion. The lesion was dilated using a 3 or 4 mm-diameter balloon, then a Wallstent™ (Boston Scientific) was deployed under distal filter protection. Angioplasty balloons with diameters ≤80% of the normal luminal diameter distal to the stenotic site were used for conservative balloon post-dilatation under distal filter protection, then removed when the procedure was completed[16]. A column of blood proximal to the filter was suctioned several times using an aspiration catheter if

the slow-flow phenomenon was recognised. All procedural symptomatic ischaemic and haemorrhagic events, and the slow-flow phenomenon were recorded. Ipsilateral and contralateral stroke (<7-day and <30-day), cardiovascular events, major adverse cardiac and cerebrovascular events (MACCE), and disease-specific mortality (DSM) for myocardial infarction and stroke within one month of CAS were also recorded during patient follow-up.

NIRS AND INTRAVASCULAR ULTRASOUND IMAGING

Both NIRS and intravascular ultrasound (IVUS) were performed utilising a single 3.2 Fr rapid-exchange Dualpro™ IVUS+NIRS imaging catheter (Infraredx Inc., Burlington, MA, USA). Catheter retraction at 0.5 mm/s was automated, and raw spectra were acquired at 40 Hz (wavelengths, 1,180-2,500 nm), to produce images with data points spaced 0.1 mm apart every 1°. The fraction of yellow pixels obtained from an image map derived from the NIRS measurements (chemogram) was multiplied by 1,000 to compute the lipid core burden index (LCBI). Therefore, the 4 mm long segment, with the maximum LCBI (max-LCBI 4 mm) ranging from 0 to 1,000 and representing the percentage of lipid core in the investigated segment, was calculated by the Makoto™ intravascular imaging system (Infraredx). Lipid signals from regions of interest (ROI) were quantified using the following parameters: maximal LCBI for any 4 mm segment in a target lesion defined as max-$LCBI_{area}$, the maximal LCBI for a segment 2 mm proximal and distal from the site of a minimal luminal area (MLA) was defined as max-$LCBI_{MLA}$, and lesion-LCBI was defined as LCBI when an entire plaque lesion defined by IVUS was included. The IVUS images were acquired via a 40 MHz transducer rotating at the same speed as the NIRS probe. Three NIRS-IVUS measurements were taken during CAS before balloon predilatation (baseline), after stent deployment, and after balloon post-dilatation. MLAs, plaque burden (PB), and calcifications were assessed using IVUS. Plaques at the MLA were defined as calcified when calcifications were visually evident.

MRI PLAQUE IMAGING AND DIFFUSION-WEIGHTED IMAGING

Plaques were also characterised by MRI using the MAGNETOM® Verio 3-T system (Siemens Healthineers, Forchheim, Germany). Two-dimensional T1-weighted (T1W) sequence images (FA:120, TR:600, TE:13) were acquired four weeks before CAS using black-blood double inversion recovery preparation and fat-saturation pulses. The signal intensity of the T1-weighted sequence was measured with the ROI drawn over carotid plaque, and the signal intensity ratio (T1W-SIR) of plaque relative to adjacent muscle was calculated. The SIR at the MLAs was defined as plaque SIR_{MLA} and maximal SIR at all stenotic lesions was defined as plaque SIR_{area}. Three-dimensional time-of-flight (TOF) MR angiography (FA:19, TR:22, TE:3.69) was also carried out four weeks before CAS. A Cohen κ value of 0.76 indicated a high level of between-observer agreement for the presence of hyperintense signals in plaque on TOF magnetic resonance angiography (MRA) images[4]. Diffusion-weighted images were acquired using multisection, single-shot, spin-echo planar imaging from 18 to 24 hrs after the CAS procedure using a MAGNETOM Verio 3-T system. The imaging parameters comprised: echo duration, 100 ms; field of view, 23 cm; intersection gap, 1 mm; matrix, 96×128; section thickness, 5 mm. Experienced neuroradiologists who were blinded to the clinical information reviewed all DWI scans and apparent diffusion coefficient (ADC) maps acquired from the patients. Ischaemic lesions which arose due to procedure-related cerebral embolisms were defined as new ipsilateral hyperintense lesions on DWI. Each individual embolus was manually traced on individual MRI slices using Synapse Vincent software (Fujifilm Medical, Tokyo, Japan), which then incorporated slice thickness and interslice gap to calculate the volume of each infarct as well as their total volume.

STATISTICAL ANALYSIS

All data are presented as means±standard deviation. Between-group comparisons were assessed using Student's tests, Fisher's exact tests and the ANOVA test. Linear regression models were used to assess the relationship between two parameters. Differences were deemed statistically significant at $p<0.05$. The diagnostic values of LCBI determined by NIRS and plaque burden determined by IVUS were assessed by calculating the area under the receiver operating characteristic (ROC) curves (AUC) for sensitivity versus 1-specificity to determine cut-offs for new ipsilateral DWI positivity after CAS. Univariate analysis was performed, and factors with a p-value <0.10 were included in the multivariate logistic regression analysis.

Results

STUDY POPULATION

Table 1 presents the clinical characteristics of the 117 enrolled patients (male, n=104; female, n=13; mean age, 75 years). The mean

Table 1. Clinical characteristics of the 117 patients.

Variable	No. of patients (%)		*p*-value
	DWI positive (n=39)	DWI negative (n=78)	
General characteristics			
Median age (range)	77 (52-90)	76 (59-89)	0.158
Females	3 (7%)	10 (13%)	0.603
Risk factor			
Hypertension	25 (64%)	60 (77%)	0.213
Diabetes	15 (42%)	36 (46%)	0.553
Current smoker	5 (13%)	5 (6%)	0.413
CKD	22 (56%)	43 (55%)	0.948
Medications			
Statins	39 (100%)	78 (100%)	1.000
ARBs	19 (49%)	47 (60%)	0.323
PPIs	9 (23%)	18 (13%)	0.816
DAPT	39 (100%)	78 (100%)	1.000

ARBs: angiotensin receptor blockers; CKD: chronic kidney disease; DAPT: dual antiplatelet therapy; DWI: diffusion-weighted imaging; PPIs: proton pump inhibitors

ages of the new ipsilateral DWI positive (n=39) and negative (n=78) groups were 77 (range, 52-90) and 75 (range, 59-89) years, respectively. Baseline characteristics, risk factors and medications did not significantly differ between the groups, but symptomatic lesions were significantly more frequent in the new ipsilateral DWI positive group than in the negative group (74% vs 53%, p=0.028) **(Table 2)**. There were four ipsilateral strokes (<7 days) and 3 of 4 patients showed slow-flow phenomenon **(Supplementary Table 1)**. **Figure 1** shows two representative patients.

NIRS WITH IVUS ASSESSMENT FOR CAROTID PLAQUE

Details can be found in **Supplementary Appendix 1** and **Supplementary Table 2**.

NIRS-DERIVED LCP AND NEW IPSILATERAL DWI POSITIVITY

A significant linear correlation was indicated between max-$LCBI_{area}$ and the number of new emboli (r=0.544, p<0.0001) and between max-$LCBI_{area}$ and the total volume of embolic lesions (r=0.473, p<0.0001) **(Figure 2A, Figure 2B)**. There were significant differences in the number of new emboli and the total volume of emboli between the groups with max-LCBI <500 and ≥500 (0.7±2.7 vs 5.0±7.0, 0.9±3.6 mm^3 vs 22.0±42.3 mm^3, p<0.001 for both) **(Figure 2C, Figure 2D)**[8]. Analyses of ROC curves for max-$LCBI_{MLA}$, max-$LCBI_{area}$, lesion-LCBI, and plaque burden showed that the max-$LCBI_{MLA}$ could be more useful to

Table 2. Comparison of lesion characteristics between groups.

Variable	No. of patients (%)		*p*-value
	DWI positive (n=39)	DWI negative (n=78)	
Lesion characteristics			
Symptomatic lesion	29 (74%)	40 (53%)	0.028*
Lesion side (left)	22 (56%)	39 (50%)	0.852
Degree of stenosis (%)	85.6±12.6	84.2±10.4	0.248
NIRS measurement			
$LCBI_{lesion}$	336.0±186.3	124.0±123.2	<0.001*
Max-$LCBI_{MLA}$	612.7±193.1	199.1±183.9	<0.001*
Max-$LCBI_{area}$	647.6±175.4	273.0±173.0	<0.001*
IVUS measurement			
MLA (mm^2)	5.6±3.6	6.3±4.0	0.366
Plaque burden (%)	82.8±10.2	82.6±9.2	0.875
Calcification	20 (51%)	51 (65.0%)	0.204
MRI plaque imaging			
T1W-SIR_{MLA}	1.9±0.3	1.8±0.6	0.593
T1W-SIR_{area}	2.1±0.5	2.1±0.8	0.956
TOF high intensity	11 (39%)	28 (47%)	0.627

*p<0.05. LCBI: lipid core burden index; MLA: minimal lesion area; T1W-SIR: T1-weighted image of signal intensity ratio; TOF: time of flight

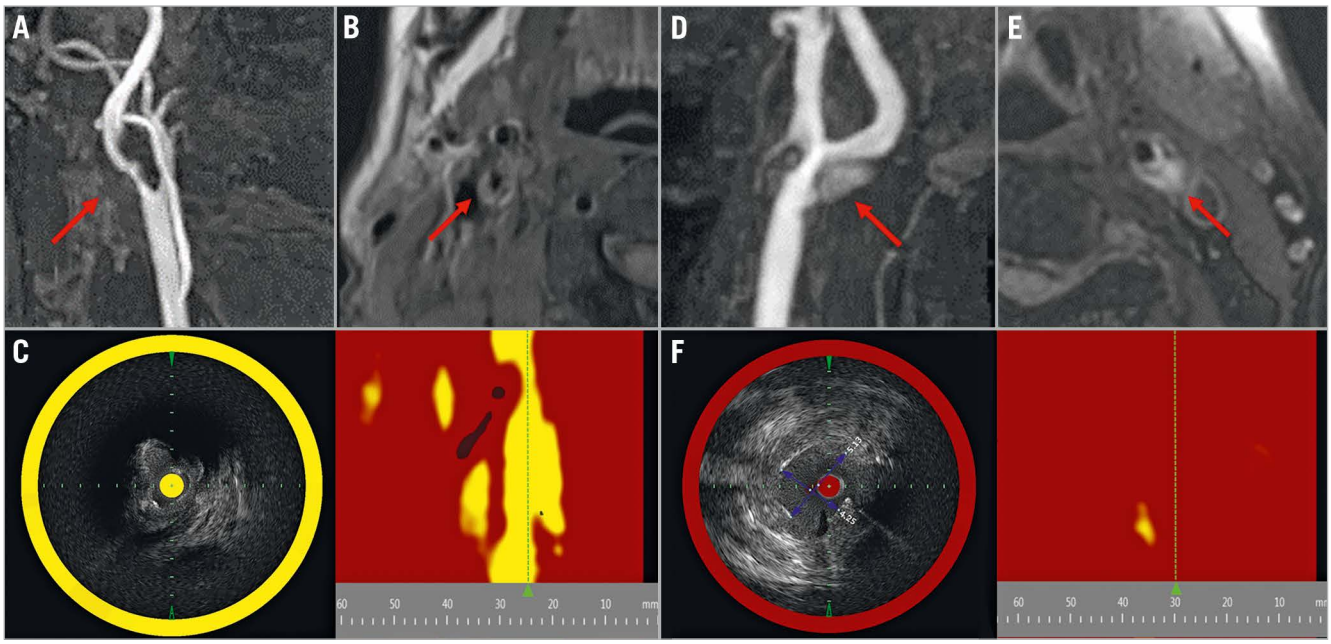

Figure 1. *Findings from NIRS-IVUS and MRI of carotid plaques. A) Right symptomatic carotid stenosis in a 79-year-old man on TOF image (arrow). B) Plaque has slightly higher intensity on the T1-weighted image (arrow). C) NIRS-IVUS has a very high LCBI (961) at the MLA segment. This patient presented with embolic stroke and stent occlusion after CAS. D) Left asymptomatic carotid stenosis in a 72-year-old man on TOF image (arrow). E) Plaque manifests as higher intensity than adjacent muscle on the T1-weighted image (arrow). F) NIRS-IVUS reveals very low LCBI (111) at the MLA segment. Embolic events did not occur after CAS in this patient. CAS: carotid artery stenting; IVUS: intravascular ultrasound; LCBI: lipid core burden index; MLA: minimal lumen area; MRA: magnetic resonance angiography; MRI: magnetic resonance imaging; NIRS: near-infrared spectroscopy; TOF: time-of-flight*

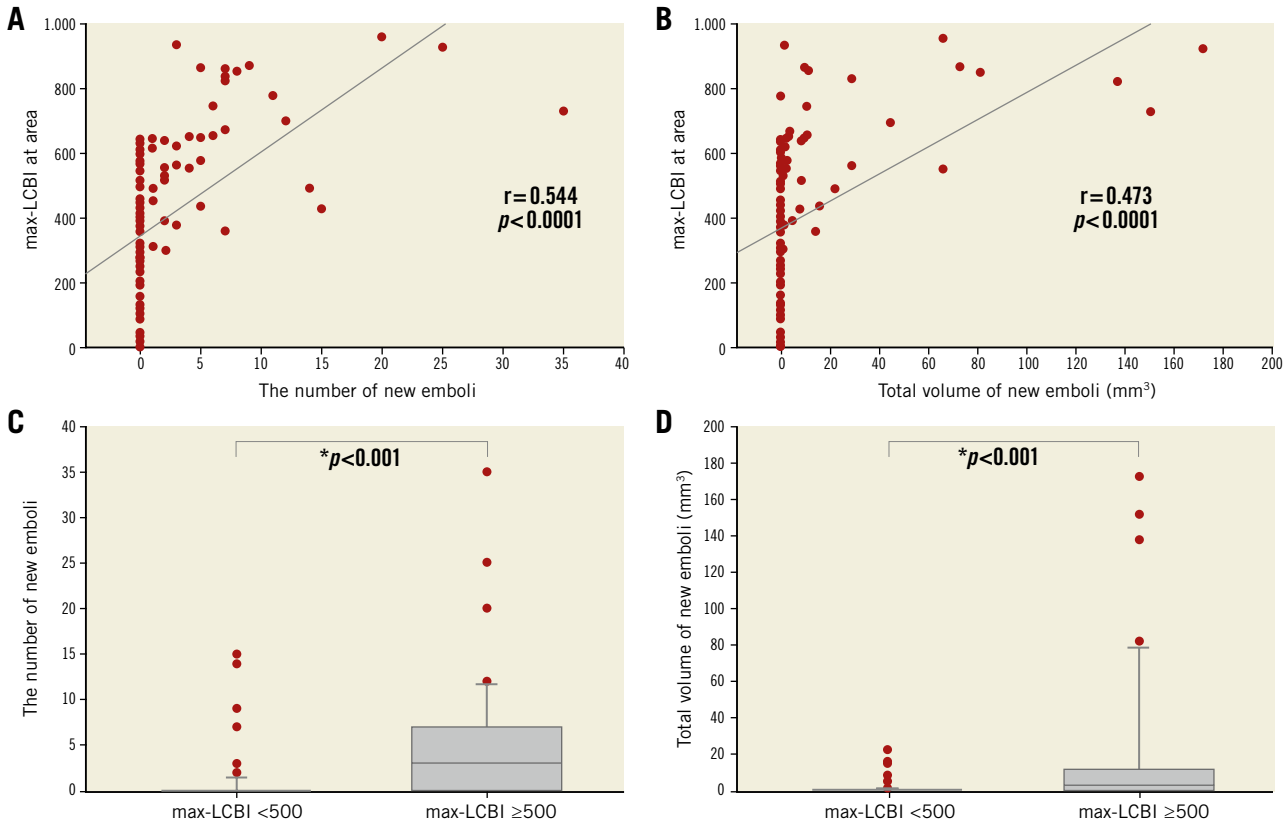

Figure 2. *Relationship between new ipsilateral emboli and LCBI. A significant linear correlation was indicated between max-LCBI$_{area}$ and the number of new emboli (A) and between max-LCBI$_{area}$ and total volume of the embolic lesion (B). There were significant differences in the number of new emboli (C) and total volume of emboli (D) between the groups with max-LCBI <500 and ≥500.*

distinguish between patients with and without postoperative new ipsilateral DWI positivity (AUC 0.91, 0.89, 0.85, 0.50, sensitivity: 0.79, 0.79, 0.73, 0.29, specificity: 0.83, 0.81, 0.85, 0.78, 95% CI: 0.86-0.96, 0.84-0.95, 0.78-0.92, 0.39-0.62, p<0.0001, <0.0001, <0.0001, 0.95, respectively) **(Figure 3)**. A max-LCBI$_{MLA}$ of ≥504 was the optimal cut-off for the risk of new ipsilateral DWI positivity. On multivariate logistic regression analysis, high LCP was the factor related to ipsilateral DWI-positive embolism (p<0.001, odds ratio 33.34, 95% CI: 8.68-128.03) **(Supplementary Table 3)**.

Discussion

The high LCP measured by NIRS was a crucial factor with which to define increased risk of ipsilateral embolic infarct during CAS, and max-LCBI$_{area}$ ≥504 was the optimal cut-off for the risk of ipsilateral embolism. A significant linear correlation was indicated between max-LCBI$_{area}$ and the number of new emboli, and the high LCP group also had a significantly higher frequency of new ipsilateral DWI positivity than the low LCP group. This first comparison with MRI showed that NIRS could identify a relationship between carotid plaque characteristics and risk of ipsilateral cerebral embolism associated with CAS. The strength of the present study is that it clearly shows an association between the carotid

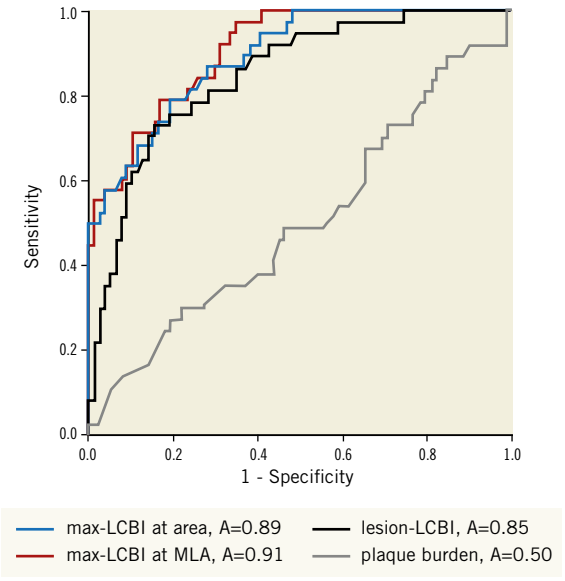

Figure 3. *Accuracy of max-LCBI and plaque burden to detect new ipsilateral emboli after CAS assessed using ROC curves. Pairwise comparisons show significantly greater AUC for max-LCBI$_{MLA}$ (red line), max-LCBI$_{area}$ (blue line), and lesion-LCBI (black line) than plaque burden (grey line). AUC: area under the ROC curve; CAS: carotid artery stenting; ROC: receiver operating characteristic*

high LCP by NIRS and cerebral DWI-positive embolism in neuroprotected CAS using a single-layer stent.

LIPID CORE OF PLAQUE ASSESSED BY NIRS AND CAS HIGH-RISK PLAQUE

The main concern during CAS is to avoid embolic infarct. Unlike CEA, CAS mechanically pushes plaque outwards, which could release plaque debris into the bloodstream. Therefore, precise evaluation of carotid plaque components is clinically important to reduce ischaemic complications. In the present study, values for max-LCBI$_{area}$ were significantly higher than those of max-LCBI$_{MLA}$ in all lesions, which indicates that the MLA is not always the site of the worst lipid-rich plaque characteristics. These results are consistent with previous reports[12,17]. IPH is one of the most dangerous features because it is significantly associated with clinical ipsilateral cerebrovascular events. However, not all plaque with IPH is associated with embolism[3,18]. Indeed, MRI and several other techniques can detect and differentiate LCP from IPH[19,20]. However, conventional MRI has limited ability to measure the volumes of these components. A catheter-based NIRS system has recently been validated for the automated identification of LCP in coronary arteries[21-24]. Recent coronary studies have found that max-LCBI >400 determined by NIRS can accurately distinguish culprit from non-culprit segments within arteries of patients with ST-segment elevation myocardial infarction (MI)[21]. Percutaneous coronary intervention of lesions with large and small (max-LCBI ≥500 and <500, respectively) lipid cores determined by NIRS is associated with 50% and 4.2% risk, respectively, of periprocedural MI[8,25]. The detection of LCP by NIRS has been validated basically in vessels with a diameter <3.5 mm, and the NIRS-IVUS technology had not been histologically validated in larger vessels; however, we have currently proved that max-LCBI assessed by NIRS showed a significant positive linear correlation with histological evaluations in carotid lesions[14]. Here, we found that a high LCP measured by NIRS is a crucial factor for defining increased risk of embolic infarct in CAS and that a max-LCBI$_{area}$ ≥504 was the optimal cut-off for the risk of ipsilateral embolism. Our results are consistent with those of previous coronary studies. Although the closed-cell design carotid artery Wallstent was used in the present study, recent optical coherence tomography assessments proved that the incidence of plaque prolapse of second-generation stents was lower than that of standard closed-cell stents[26,27]. The incidence of plaque prolapse of the single-layer stents (including closed-cell) is substantial, and only significantly reduced with two overlapped closed-cell stents[26]. The dual-layer carotid artery stent constitutes a second generation, where the MicroNet® mesh-covered stent (InspireMD, Tel Aviv, Israel) has demonstrated superiority versus the Roadsaver® stent (Terumo Corp., Tokyo, Japan)[27]. In contrast, an increased occupation ratio of IPH is more closely associated with the development of microembolic signals than the occupation ratio of LCP during CEA[28,29]. These results indicate that lipid-predominant plaque could be an embolic risk factor during CAS and that IPH-predominant plaque could be an embolic risk factor during CEA. If high embolic risk could be considered by NIRS as a high LCP in the clinical context, mesh-covered or dual-layer carotid stents could be deployed[30], double filtration devices could be applied, and treatment strategies could be changed from CAS to CEA.

LIPID CORE OF PLAQUE ASSESSED BY NIRS AND INTRAPLAQUE HAEMORRHAGE

Details can be found in **Supplementary Appendix 2**.

Limitations

The small sample assessed at a single institution limited the statistical power and might have introduced bias into patient selection, data collection, and clinical outcomes. Therefore, the present results cannot be translated directly into clinical decision making. The other limitation is the lack of analysis of embolism parameters including the mean, total volume of LCPs, the length of LCPs, and the lack of 30-day imaging analysis. Although plaque evaluation by catheter-based NIRS is a relatively invasive imaging technique, it could be an additional modality to discriminate LCP at high risk for cerebral embolism by diffusion-weighted imaging during CAS. Standard closed-cell stents were used with a distal filter embolic protection device in the present study; however, usage of second-generation stents under flow reversal with Mo.Ma™ (Medtronic, Minneapolis, MN, USA) and transcarotid artery revascularisation (TCAR) could further reduce the incidence of new ipsilateral emboli[31-33]. Further work is needed to confirm whether optimised plaque insulation with new-generation (double-layer) carotid stents abolishes the association between the NIRS highly lipidic plaque characteristics and periprocedural cerebral embolism in neuroprotected CAS.

Conclusions

High LCP assessed by NIRS is associated with cerebral embolism by diffusion-weighted imaging in CAS.

Impact on daily practice

Large lipid core detected by NIRS was associated with an increased risk of cerebral embolism using a first-generation (single-layer) stent. This risk might be mitigated by selecting a second-generation (such as MicroNet-covered) carotid artery stent rather than a single-layer stent and strengthening the peri-CAS hypolipidaemic and antithrombotic therapy.

Conflict of interest statement

The authors have no conflicts of interest to declare.

References

1. Brott TG, Calvet D, Howard G, Gregson J, Algra A, Becquemin JP, de Borst GJ, Bulbulia R, Eckstein HH, Fraedrich G, Greving JP, Halliday A, Hendrikse J, Jansen O, Voeks JH, Ringleb PA, Mas JL, Brown MM, Bonati LH; Carotid Stenosis Trialists'

Collaboration. Long-term outcomes of stenting and endarterectomy for symptomatic carotid stenosis: a preplanned pooled analysis of individual patient data. *Lancet Neurol.* 2019;18:348-56.

2. Kotsugi M, Takayama K, Myouchin K, Wada T, Nakagawa I, Nakagawa H, Taoka T, Kurokawa S, Nakase H, Kichikawa K. Carotid Artery Stenting: Investigation of Plaque Protrusion Incidence and Prognosis. *JACC Cardiovasc Interv.* 2017;10: 824-31.

3. Saba L, Saam T, Jäger HR, Yuan C, Hatsukami TS, Saloner D, Wasserman BA, Bonati LH, Wintermark M. Imaging biomarkers of vulnerable carotid plaques for stroke risk prediction and their potential clinical implications. *Lancet Neurol.* 2019;18:559-72.

4. Yoshimura S, Yamada K, Kawasaki M, Asano T, Kanematsu M, Takamatsu M, Hara A, Iwama T. High-intensity signal on time-of-flight magnetic resonance angiography indicates carotid plaques at high risk for cerebral embolism during stenting. *Stroke.* 2011;42:3132-7.

5. Zhou W, Baughman BD, Soman S, Wintermark M, Lazzeroni LC, Hitchner E, Bhat J, Rosen A. Volume of subclinical embolic infarct correlates to long-term cognitive changes after carotid revascularization. *J Vasc Surg.* 2017;65:686-94.

6. Traenka C, Engelter ST, Brown MM, Dobson J, Frost C, Bonati LH. Silent brain infarcts on diffusion-weighted imaging after carotid revascularisation: A surrogate outcome measure for procedural stroke? A systematic review and meta-analysis. *Eur Stroke J.* 2019;4:127-43.

7. Yuan C, Mitsumori LM, Ferguson MS, Polissar NL, Echelard D, Ortiz G, Small R, Davies JW, Kerwin WS, Hatsukami TS. In vivo accuracy of multispectral magnetic resonance imaging for identifying lipid-rich necrotic cores and intraplaque hemorrhage in advanced human carotid plaques. *Circulation.* 2001;104:2051-6.

8. Goldstein JA, Maini B, Dixon SR, Brilakis ES, Grines CL, Rizik DG, Powers ER, Steinberg DH, Shunk KA, Weisz G, Moreno PR, Kini A, Sharma SK, Hendricks MJ, Sum ST, Madden SP, Muller JE, Stone GW, Kern MJ. Detection of lipid-core plaques by intracoronary near-infrared spectroscopy identifies high risk of periprocedural myocardial infarction. *Circ Cardiovasc Interv.* 2011;4:429-37.

9. Chung GH, Jeong JY, Kwak HS, Hwang SB. Associations between Cerebral Embolism and Carotid Intraplaque Hemorrhage during Protected Carotid Artery Stenting. *AJNR Am J Neuroradiol.* 2016;37:686-91.

10. Oemrawsingh RM, Cheng JM, García-García HM, van Geuns RJ, de Boer SP, Simsek C, Kardys I, Lenzen MJ, van Domburg RT, Regar E, Serruys PW, Akkerhuis KM, Boersma E; ATHEROREMO-NIRS Investigators. Near-infrared spectroscopy predicts cardiovascular outcome in patients with coronary artery disease. *J Am Coll Cardiol.* 2014;64:2510-8.

11. Waksman R, Di Mario C, Torguson R, Ali ZA, Singh V, Skinner WH, Artis AK, Cate TT, Powers E, Kim C, Regar E, Wong SC, Lewis S, Wykrzykowska J, Dube S, Kazziha S, van der Ent M, Shah P, Craig PE, Zou Q, Kolm P, Brewer HB, Garcia-Garcia HM; LRP Investigators. Identification of patients and plaques vulnerable to future coronary events with near-infrared spectroscopy intravascular ultrasound imaging: a prospective, cohort study. *Lancet.* 2019;394:1629-37.

12. Štěchovský C, Hájek P, Horváth M, Špaček M, Veselka J. Near-infrared spectroscopy combined with intravascular ultrasound in carotid arteries. *Int J Cardiovasc Imaging.* 2016;32:181-8.

13. Štěchovský C, Hájek P, Horváth M, Veselka J. Effect of stenting on the near-infrared spectroscopy-derived lipid core burden index of carotid artery plaque. *EuroIntervention.* 2019;15:e289-96.

14. Kotsugi M, Nakagawa I, Hatakeyama K, Park H, Sato F, Furuta T, Nishimura F, Yamada S, Motoyama Y, Park YS, Nakase H. Lipid Core Plaque Distribution Using Near Infrared Spectroscopy Is Consistent With Pathological Evaluation In Carotid Artery Plaques. *Neurol Med Chir (Tokyo).* 2020;60:499-506.

15. Gurm HS, Yadav JS, Fayad P, Katzen BT, Mishkel GJ, Bajwa TK, Ansel G, Strickman NE, Wang H, Cohen SA, Massaro JM, Cutlip DE; SAPPHIRE Investigators. Long-term results of carotid stenting versus endarterectomy in high-risk patients. *N Engl J Med.* 2008;358:1572-9.

16. Lauricella A, Berchiolli R, Moratto R, Ferri M, Viazzo A, Silingardi R. Impact of plaque dilation before carotid artery stent deployment. *J Vasc Surg.* 2020;71:842-53.

17. Sangiorgi G, Bedogni F, Sganzerla P, Binetti G, Inglese L, Musialek P, Esposito G, Cremonesi A, Biasi G, Jakala J, Mauriello A, Biondi-Zoccai G. The Virtual histology In CaroTids Observational RegistrY (VICTORY) study: a European prospective registry to assess the feasibility and safety of intravascular ultrasound and virtual histology during carotid interventions. *Int J Cardiol.* 2013;168:2089-93.

18. Wang X, Sun J, Zhao X, Hippe DS, Hatsukami TS, Liu J, Li R, Canton G, Song Y, Yuan C; CARE-II study investigators. Ipsilateral plaques display higher T1 signals than contralateral plaques in recently symptomatic patients with bilateral carotid intraplaque hemorrhage. *Atherosclerosis.* 2017;257:78-85.

19. Brinjikji W, Huston J 3rd, Rabinstein AA, Kim GM, Lerman A, Lanzino G. Contemporary carotid imaging: from degree of stenosis to plaque vulnerability. *J Neurosurg.* 2016;124:27-42.

20. Narumi S, Sasaki M, Ohba H, Ogasawara K, Kobayashi M, Natori T, Hitomi J, Itagaki H, Takahashi T, Terayama Y. Predicting carotid plaque characteristics using quantitative color-coded T1-weighted MR plaque imaging: correlation with carotid endarterectomy specimens. *AJNR Am J Neuroradiol.* 2014;35:766-71.

21. Gardner CM, Tan H, Hull EL, Lisauskas JB, Sum ST, Meese TM, Jiang C, Madden SP, Caplan JD, Burke AP, Virmani R, Goldstein J, Muller JE. Detection of lipid core coronary plaques in autopsy specimens with a novel catheter-based near-infrared spectroscopy system. *JACC Cardiovasc Imaging.* 2008;1:638-48.

22. Waxman S, Dixon SR, L'Allier P, Moses JW, Petersen JL, Cutlip D, Tardif JC, Nesto RW, Muller JE, Hendricks MJ, Sum ST, Gardner CM, Goldstein JA, Stone GW, Krucoff MW. In vivo validation of a catheter-based near-infrared spectroscopy system for detection of lipid core coronary plaques: initial results of the SPECTACL study. *JACC Cardiovasc Imaging.* 2009;2:858-68.

23. Brilakis ES, Banerjee S. How to detect and treat coronary fibroatheromas: the synergy between IVUS and NIRS. *JACC Cardiovasc Imaging.* 2015;8:195-7.

24. Kang SJ, Mintz GS, Pu J, Sum ST, Madden SP, Burke AP, Xu K, Goldstein JA, Stone GW, Muller JE, Virmani R, Maehara A. Combined IVUS and NIRS detection of fibroatheromas: histopathological validation in human coronary arteries. *JACC Cardiovasc Imaging.* 2015;8:184-94.

25. Kini AS, Motoyama S, Vengrenyuk Y, Feig JE, Pena J, Baber U, Bhat AM, Moreno P, Kovacic JC, Narula J, Sharma SK. Multimodality Intravascular Imaging to Predict Periprocedural Myocardial Infarction During Percutaneous Coronary Intervention. *JACC Cardiovasc Interv.* 2015;8:937-45.

26. Harada K, Oshikata S, Kajihara M. Optical coherence tomography evaluation of tissue prolapse after carotid artery stenting using closed cell design stents for unstable plaque. *J Neurointerv Surg.* 2018;10:229-34.

27. Umemoto T, de Donato G, Pacchioni A, Reimers B, Ferrante G, Isobe M, Setacci C. Optical coherence tomography assessment of newgeneration mesh-covered stents after carotid stenting. *EuroIntervention.* 2017;13:1347-54.

28. Altaf N, Beech A, Goode SD, Gladman JR, Moody AR, Auer DP, MacSweeney ST. Carotid intraplaque hemorrhage detected by magnetic resonance imaging predicts embolization during carotid endarterectomy. *J Vasc Surg.* 2007; 46:31-6.

29. Sato Y, Ogasawara K, Narumi S, Sasaki M, Saito A, Tsushima E, Namba T, Kobayashi M, Yoshida K, Terayama Y, Ogawa A. Optimal MR Plaque Imaging for Cervical Carotid Artery Stenosis in Predicting the Development of Microembolic Signals during Exposure of Carotid Arteries in Endarterectomy: Comparison of 4 T1-Weighted Imaging Techniques. *AJNR Am J Neuroradiol.* 2016;37:1146-54.

30. Stabile E, de Donato G, Musialek P, De Loose K, Nerla R, Sirignano P, Chianese S, Mazurek A, Tesorio T, Bosiers M, Setacci C, Speziale F, Micari A, Esposito G. Use of Dual-Layered Stents in Endovascular Treatment of Extracranial Stenosis of the Internal Carotid Artery: Results of a Patient-Based Meta-Analysis of 4 Clinical Studies. *JACC Cardiovasc Interv.* 2018;11:2405-11.

31. Hornung M, Bertog SC, Franke J, Id D, Grunwald I, Sievert H. Evaluation of proximal protection devices during carotid artery stenting as the first choice for embolic protection. *EuroIntervention.* 2015;10:1362-7.

32. Malas MB, Leal Lorenzo JI, Nejim B, Hanover TM, Mehta M, Kashyap V, Kwolek CJ, Cambria R. Analysis of the ROADSTER pivotal and extended-access cohorts shows excellent 1-year durability of transcarotid stenting with dynamic flow reversal. *J Vasc Surg.* 2019;69:1786-96.

33. Schofer J, Musiałek P, Bijuklic K, Kolvenbach R, Trystula M, Siudak Z, Sievert H. Prospective, Multicenter Study of a Novel Mesh-Covered Carotid Stent: The CGuard CARENET Trial (Carotid Embolic Protection Using MicroNet). *JACC Cardiovasc Interv.* 2015;8:1229-34.

34. Altaf N, MacSweeney ST, Gladman J, Auer DP. Carotid intraplaque hemorrhage predicts recurrent symptoms in patients with high-grade carotid stenosis. *Stroke.* 2007;38:1633-5.

35. Chu B, Kampschulte A, Ferguson MS, Kerwin WS, Yarnykh VL, O'Brien KD, Polissar NL, Hatsukami TS, Yuan C. Hemorrhage in the atherosclerotic carotid plaque: a high-resolution MRI study. *Stroke.* 2004;35:1079-84.

36. Moody AR, Murphy RE, Morgan PS, Martel AL, Delay GS, Allder S, MacSweeney ST, Tennant WG, Gladman J, Lowe J, Hunt BJ. Characterization of complicated carotid plaque with magnetic resonance direct thrombus imaging in patients with cerebral ischemia. *Circulation.* 2003;107:3047-52.

37. Saito A, Sasaki M, Ogasawara K, Kobayashi M, Hitomi J, Narumi S, Ohba H, Yamaguchi M, Kudo K, Terayama Y. Carotid plaque signal differences among four kinds of T1-weighted magnetic resonance imaging techniques: a histopathological correlation study. *Neuroradiology.* 2012;54:1187-94.

38. Yang D, Liu Y, Han Y, Li D, Wang W, Li R, Yuan C, Zhao X. Signal of Carotid Intraplaque Hemorrhage on MR T1-Weighted Imaging: Association with Acute Cerebral Infarct. *AJNR Am J Neuroradiol.* 2020;41:836-43.

39. Narumi S, Sasaki M, Ohba H, Ogasawara K, Kobayashi M, Hitomi J, Mori K, Ohura K, Yamaguchi M, Kudo K, Terayama Y. Prediction of carotid plaque characteristics using non-gated MR imaging: correlation with endarterectomy specimens. *AJNR Am J Neuroradiol.* 2013;34:191-7.

Supplementary data

Supplementary Appendix 1. NIRS with IVUS assessment for carotid plaque.

Supplementary Appendix 2. Lipid core of plaque assessed by NIRS and intraplaque haemorrhage.

Supplementary Table 1. Carotid artery stenting and clinical outcomes.

Supplementary Table 2. Lesion characteristics and DWI positivity among three quantiles (n=39 each).

Supplementary Table 3. Logistic regression analysis for factors related to DWI-positive embolism.

The supplementary data are published online at: https://eurointervention.pcronline.com/doi/10.4244/EIJ-D-20-01050

Supplementary data

Supplementary Appendix 1. NIRS with IVUS assessment for carotid plaque

There were no NIRS-IVUS related complications in the present study. Parameters associated with IVUS including MLA, plaque burden and calcification did not differ significantly; however, values for lesion-LCBI, max-$LCBI_{MLA}$ and max-$LCBI_{area}$ were significantly higher in the new ipsilateral DWI positive group, than in the negative group (336.0±186.3 vs 124.0±123.2, 612.7±193.1 vs 199.1±183.9 and 647.6±175.4 vs 273.0±173.0, respectively; $p<0.001$ for all) **(Table 2)**. Values for max-$LCBI_{area}$ were significantly higher than those of max-$LCBI_{MLA}$ in all lesions (397.9±47.8 vs 338.1±270.5, respectively; $p=0.036$). Furthermore, the patients were equally divided (n=39 each) into three quantiles (Q1, 2 and 3; based on T1W-SIR_{MLA} of MR plaque imaging and mean SIR of 1.30 [0.95–1.66], 1.93 [1.68–2.15] and 2.82 [2.17–3.08], respectively). The frequency of new ipsilateral DWI positivity, number and total volume was significantly higher in Q2 than in Q1 and Q3. In contrast, the frequency of TOF high intensity was significantly higher in Q3 than in Q1 and Q2 **(Supplementary Table 2)**.

Supplementary Appendix 2. Lipid core of plaque assessed by NIRS and intraplaque haemorrhage

Recent developments in MRI with high-contrast resolution have enabled non-invasive assessment of carotid plaque vulnerability[34-36]. IPH manifesting as a high-signal intensity ratio is closely associated with ischaemic events in symptomatic patients[37,38]; however, IPH was not a significant risk factor for cerebral embolism during CAS in patients with severe carotid stenosis[9]. Therefore, we found significantly high max-LCBI in Q2, which also had a significantly high frequency of new ipsilateral DWI positivity compared with Q1 and Q3. Recent non-gated T1-weighted plaque MRI has indicated that the median (range) contrast ratios among carotid plaques comprising mainly fibrous tissue, or lipid/necrosis and haemorrhage were 0.97 (0.54–1.17), 1.27 (1.16–1.53) and 1.99 (1.40–2.29), respectively, with a small overlap and high sensitivity and specificity[20,39]. The present results are consistent with these findings. We presumed that the low LCBI in the low (Q1) and high (Q3) T1W-SIR ranges was due to a high ratio of fibrous tissue, and to high ratios of IPH, respectively. These results are consistent with a previous report that IPH was not a significant risk factor for cerebral embolism during CAS[9]. Moreover, ROC curve analyses indicated that max-LCBI determined by NIRS could effectively distinguish patients with postoperative new ipsilateral DWI positivity with high sensitivity and specificity. These results still indicate that high LCP is a crucial risk factor involved in embolic infarct by diffusion-weighted imaging during CAS, whereas IPH is not.

Supplementary Table 1. Carotid artery stenting and clinical outcomes.

Variable	No. of patients (%)	
	DWI positive (n=39)	DWI negative (n=78)
CAS procedure		
Filter EPD	39 (100%)	78 (100%)
with flow reversal*	12 (31%)	20 (26%)
post-MLA (mm2)	9.7±4.4	10.1±3.7
Procedural events		
Slow flow	3 (8%)	0 (0%)
Ipsilateral ischaemic events	2 (5%)	0 (0%)
Contralateral ischaemic events	0 (0%)	0 (0%)
Haemorrhagic events	0 (0%)	0 (0%)
Clinical outcomes		
Ipsilateral stroke (<7 days)	4 (10%)	0 (0%)
Contralateral stroke (<7 days)	0 (0%)	0 (0%)
Ipsilateral stroke (<30 days)	4 (10%)	0 (0%)
Contralateral stroke (<30 days)	0 (0%)	0 (0%)
Cardiovascular events	0 (0%)	0 (0%)
MACCE	3 (8%)	0 (0%)
DSM	0 (0%)	0 (0%)

CAS: carotid artery stenting; DSM: disease specific mortality; DWI: diffusion weighted image; EPD: embolic protection device; MACCE: major adverse cardiac and cerebrovascular events; Post-MLA: minimal lumen area after balloon post-dilatation. *Flow reversal was applied only initially crossing the stenotic lesion over 95%.

Supplementary Table 2. Lesion characteristics and DWI positivity among three quantiles (n=39 each).

Variable	No. of patients (%)			
	Quantile 1 (n=39)	Quantile 2 (n=39)	Quantile 3 (n=39)	*p*-value
Lesion characteristics				
Symptomatic lesion	16 (41%)	30 (77%)	23 (59%)	0.006*
Lesion side (left)	18 (46%)	21 (54%)	22 (56%)	0.641
Degree of stenosis (%)	85.1±11.1	86.1±10.7	82.8±12.2	0.423
NIRS measurement				
$LCBI_{lesion}$	116.8±122.9	375.0±176.5	109.5±93.3	<0.001*
Max-$LCBI_{MLA}$	222.2±204.3	591.1±234.6	196.8±175.1	<0.001*
Max-$LCBI_{area}$	299.2±218.6	625.9±195.4	277.9±153.3	<0.001*
IVUS measurement				
MLA (mm^2)	5.9±3.4	5.8±5.1	7.2±5.4	0.264
Plaque burden (%)	82.6±10.5	83.3±10.4	81.7±9.2	0.559
Calcification	23 (59%)	24 (62%)	23 (59%)	0.965
MRI plaque imaging				
T1W-SIR_{MLA}	1.3 ± 0.2	1.9 ± 0.2	2.8±0.3	<0.001*
T1W-SIR_{area}	1.5±0.4	2.2 ± 0.4	2.7± 0.6	<0.001*
TOF high intensity	9 (23%)	18 (46%)	31 (79%)	<0.001*
MRI DWI bright lesion				
Positivity	4 (10%)	27 (69%)	8 (21%)	<0.001*
Number	0.4 ± 1.3	7.1 ± 13.6	1.2±3.4	<0.001*
Maximum size (mm^3)	0.1 ± 0.7	9.5 ± 18.3	0.4±1.2	<0.001*
Total volume (mm^3)	0.4 ± 1.7	24.0 ± 44.0	1.5±4.5	<0.001*

CAS: carotid artery stenting; DWI: diffusion weighted imaging; LCBI; lipid core burden index; MLA; minimal lesion area; T1W-SIR: T1-weighted image of signal intensity ratio ; TOF: time of flight; *: p<0.05

Supplementary Table 3. Logistic regression analysis for factors related to DWI-positive embolism.

	Univariate		Multivariate	
	p-value	OR (95% CI)	*p*-value	OR (95% CI)
Age (>75)	0.625	0.821 (0.373-1.808)	-	-
Females	0.541	1.437 (0.426-4.843)	-	-
Hypertension	0.056	0.450 (0.182-1.111)	-	-
Diabetes	0.167	0.597 (0.275-1.296)	-	-.
Current smoker	0.860	1.000 (0.317-3.157)	-	-
CKD	0.943	1.000 (0.463-2.162)	-	-
ARBs	0.106	0.508 (0.228-1.134)	-	-
PPIs	0.106	0.803 (0.143-1.039)	-	-
Symptomatic	0.030*	2.368 (1.051-5.335)	-	-
Severe stenosis	0.130	1.765 (0.812-3.835)	-	-
Calcification	0.625	0.805 (0.366-1.770)	-	-
High LCP	<0.001*	12.708 (5.033-32.089)	<0.001*	33.34 (8.68-128.03)

ARBs: angiotensin receptor blockers; CKD: chronic kidney disease; LCP: lipid core plaque; PPIs: proton pump inhibitors. High LCP cut off values were 504 of max-$LCBI_{MLA}$ defined by receiver operating characteristic curve analysis for DWI-positive embolism. *: $p<0.05$,